# Design of a Ruthenium−Cytochrome *c* Derivative To Measure Electron Transfer to the Radical Cation and Oxyferryl Heme in Cytochrome *c* Peroxidase†

Kefei Wang,‡ Hongkang Mei,‡ Lois Geren,‡ Mark A. Miller,§ Aleister Saunders,|| Xuming Wang,|| Jennifer L. Waldner,|| Gary J. Pielak,|| Bill Durham,‡ and Francis Millett*,‡

*Department of Chemistry and Biochemistry, University of Arkansas, Fayetteville, Arkansas 72701, Department of Chemistry, University of California at San Diego, La Jolla, California 92903, and Departments of Chemistry and Biochemistry and Biophysics, University of North Carolina, Chapel Hill, North Carolina 27599-3290*

*Received May 9, 1996; Revised Manuscript Received August 15, 1996*⊗

ABSTRACT: A new ruthenium-labeled cytochrome *c* derivative was designed to measure the actual rate of electron transfer to the Trp-191 radical cation and the oxyferryl heme in cytochrome *c* peroxidase compound I {CMPI($Fe^{IV}$═O,$R^{•+}$)}. The H39C,C102T variant of yeast iso-1-cytochrome *c* was labeled at the single cysteine residue with a tris(bipyridyl)ruthenium(II) reagent to form Ru-39-Cc. This derivative has the same reactivity with CMPI as native yCc measured by stopped-flow spectroscopy, indicating that the ruthenium group does not interfere with the interaction between the two proteins. Laser excitation of the 1:1 Ru-39-Cc−CMPI complex in low ionic strength buffer (2 mM phosphate, pH 7) resulted in electron transfer from $Ru^{II*}$ to heme *c* $Fe^{III}$ with a rate constant of $5 \times 10^5$ $s^{-1}$, followed by electron transfer from heme *c* $Fe^{II}$ to the Trp-191 indolyl radical cation in CMPI($Fe^{IV}$═O,$R^{•+}$) with a rate constant of $k_{eta} = 2 \times 10^6$ $s^{-1}$. A subsequent laser flash led to electron transfer from heme *c* to the oxyferryl heme in CMPII-($Fe^{IV}$═O,R) with a rate constant of $k_{etb} = 5000$ $s^{-1}$. The location of the binding domain was determined using a series of surface charge mutants of CcP. The mutations D34N, E290N, and A193F each decreased the values of $k_{eta}$ and $k_{etb}$ by 2−4-fold, consistent with the use of the binding domain identified in the crystal structure of the yCc−CcP complex for reduction of both redox centers [Pelletier, H., & Kraut, J. (1992) *Science 258,* 1748−1755]. A mechanism is proposed for reduction of the oxyferryl heme in which internal electron transfer in CMPII($Fe^{IV}$═O,R) leads to the regeneration of the radical cation in CMPII-($Fe^{III}$,$R^{•+}$), which is then reduced by $yCc^{II}$. Thus, both steps in the complete reduction of CMPI involve electron transfer from $yCc^{II}$ to the Trp-191 radical cation using the same binding site and pathway. Comparison of the rate constant $k_{eta}$ with theoretical predictions indicate that the electron transfer pathway identified in the crystalline yCc−CcP complex is very efficient. Stopped-flow studies indicate that native $yCc^{II}$ initially reduces the Trp-191 radical cation in CMPI with a second-order rate constant $k_a$, which increases from $1.8 \times 10^8$ $M^{-1}$ $s^{-1}$ at 310 mM ionic strength to $>3 \times 10^9$ $M^{-1}$ $s^{-1}$ at ionic strengths below 100 mM. A second molecule of $yCc^{II}$ then reduces the oxyferryl heme in CMPII with a second-order rate constant $k_b$ which increases from $2.7 \times 10^7$ $M^{-1}$ $s^{-1}$ at 310 mM ionic strength to $2.5 \times 10^8$ $M^{-1}$ $s^{-1}$ at 160 mM ionic strength. As the ionic strength is decreased below 100 mM the rate constant for reduction of the oxyferryl heme becomes progressively slower as the reaction is limited by release of the product $yCc^{III}$ from the $yCc^{III}$−CMPII complex. Both ruthenium photoreduction studies and stopped-flow studies demonstrate that the Trp-191 radical cation is the initial site of reduction in CMPI under all conditions of ionic strength.

The electron transfer reaction between two redox proteins typically involves at least three distinct steps: (1) formation of a complex between the two proteins, (2) electron transfer within the complex, and (3) dissociation of the product complex. The overall reaction can be rate-limited by any one of these three steps, depending on experimental conditions. Intracomplex electron transfer, step 2, is probably the most difficult to access experimentally because it is usually very rapid, and only a limited number of techniques are available for the measurement. In addition, very few protein−protein complexes have been structurally characterized with sufficient resolution to allow theoretical predictions of the rate of electron transfer. The reaction between yeast iso-1-cytochrome *c* (yCc)[1] and cytochrome *c* peroxidase (CcP) is a prototype for this problem. The resting ferric state of CcP is oxidized by hydrogen peroxide to CMPI-($Fe^{IV}$═O,$R^{•+}$), which contains an oxyferryl heme, $Fe^{IV}$═O, and a radical cation, $R^{•+}$, located on the indole group of Trp-191 (Mauro et al., 1988; Scholes et al., 1989; Erman et al., 1989; Sivaraja et al., 1989; Miller et al., 1994a; Fitzgerald et al., 1994; Huyett et al., 1995). The radical cation and oxyferryl heme in CMPI are then sequentially reduced by two molecules of $Cc^{II}$. Pelletier and Kraut (1992) determined the X-ray crystal structure of the 1:1 complex between yCc

† This work was supported in part by NIH Grants GM20488 to B.D. and F.M. and GM 52501 to G.J.P., and NSF Grant MCB 9119292 to M.A.M. and J. Kraut.

‡ University of Arkansas.
§ University of California at San Diego.
|| University of North Carolina.

⊗ Abstract published in *Advance ACS Abstracts,* November 1, 1996.

[1] Abbreviations: Cc, cytochrome *c*; hCc, horse Cc; yCc, yeast iso-1-Cc; CcP, cytochrome *c* peroxidase; CcP(MI), recombinant CcP prepared by the method of Fishel et al. (1987); CMPI, CcP compound I; CMPII, CcP compound II; Ru-39-yCc, $Ru(bpy)_2$(4,4′-dimethylbipyridine-Cys-39-(H39C;C102T)-yeast-iso-1-cytochrome *c*).

S0006-2960(96)01111-7 CCC: $12.00 

Scheme 1

$$\text{CMPI}(Fe^{IV}{=}O, R^{\bullet+}) + Cc^{II} \xrightarrow{k_a} \text{CMPII}(Fe^{IV}{=}O, R) + Cc^{III}$$

$$\text{CMPII}(Fe^{IV}{=}O, R) + 2H^+ \underset{}{\overset{K}{\rightleftharpoons}} \text{CMPII}(Fe^{III}, R^{\bullet+}) + H_2O$$

$$\text{CMPII}(Fe^{III}, R^{\bullet+}) + Cc^{II} \xrightarrow{k_a} \text{CcP}(Fe^{III}, R) + Cc^{III}$$

and CcP at physiological ionic strength and found that the exposed heme edge of yCc is in van der Waals contact with CcP residues Ala-193 and Ala-194 at the center of the binding domain. They proposed an electron transfer pathway that extends from the yCc heme methyl group through CcP residues Ala-194, Ala-193, and Gly-192 to the indole group on Trp-191, which is in van der Waals contact with the heme group. An important goal is to measure the rate of intracomplex electron transfer from $yCc^{II}$ to the radical cation and oxyferryl heme in CMPI and to determine whether the binding site and electron transfer pathway identified in the crystalline complex are used for the reaction in solution.

We have introduced a new method to measure rapid interprotein electron transfer reactions utilizing a tris(bipyridine)ruthenium complex covalently attached to Cc (Geren et al., 1991; Hahm et al., 1992). Photoexcitation of the Ru−Cc derivative leads to formation of the metal-to-ligand charge transfer state, $Ru^{II*}$, which is a strong reducing agent and rapidly transfers an electron to the Cc ferric heme (Durham et al., 1989). Six different horse and yeast Ru−Cc derivatives were found to initially reduce the radical cation in CMPI($Fe^{IV}$=O,$R^{\bullet+}$) with intracomplex rate constants ranging up to $6 \times 10^4$ $s^{-1}$ or greater at low ionic strength (Geren et al., 1991; Hahm et al., 1992). CMPII($Fe^{IV}$=O,R) is then converted to CMPII($Fe^{III}$,$R^{\bullet+}$) by intramolecular electron transfer, as shown in Scheme 1. Liu et al. (1994) found that both the rate constant and equilibrium constant $K$ for this interconversion are pH-dependent. $K$ decreases from 1.2 at pH 5.0 to 0.15 at pH 7.0, in agreement with the equilibrium studies of Coulson et al. (1971). A second molecule of Ru−$Cc^{II}$ then reduces the radical cation in CMPII($Fe^{III}$,$R^{\bullet+}$) to give the resting enzyme. Both native horse and yeast $Cc^{II}$ have been shown to reduce CMPI according to Scheme 1 at high ionic strength where the bimolecular reactions are slow enough to be measured by stopped-flow spectroscopy (Hahm et al., 1993, 1994; Miller et al., 1994b; Nuevo et al., 1993; Matthis et al., 1995). As the ionic strength is decreased, the second-order rate constants increase until they become too fast to measure by stopped-flow spectroscopy, but the initial electron acceptor in CMPI remains the radical cation (Hahm et al., 1993, 1994; Miller et al., 1994b). The reaction sequence shown in Scheme 1 is consistent with the use of the binding domain identified in the crystalline yCc−CcP and hCc−CcP complexes (Pelletier & Kraut, 1992). Both interprotein reactions in Scheme 1 involve electron transfer from $Cc^{II}$ to the Trp-191 radical cation using the Pelletier−Kraut binding domain (Miller et al., 1994b). However, Erman and co-workers reported that when excess yeast or horse $Cc^{II}$ is mixed with CMPI at low ionic strength in the stopped-flow spectrometer, the oxyferryl heme is initially reduced, followed by very slow reduction of the radical cation in CMPII($Fe^{III}$,$R^{\bullet+}$) (Matthis et al., 1995; Nuevo et al., 1993). Hazzard et al. (1987) and Hazzard and Tollin (1991) also reported initial reduction of the oxyferryl heme in CMPI using a flash photolysis method to generate $Cc^{II}$. Mechanisms involving initial reduction of the oxyferryl heme do not appear to be compatible with the use of the binding domain in the crystalline yCc−CcP complex because Trp-191 is located between the hemes of yCc and CcP, and reduction of the Trp-191 indolyl radical cation is thermodynamically more favorable than the oxyferryl heme at pH 7 and above (Coulson et al., 1971).

For this study we have utilized a new yeast Ru−Cc derivative specifically designed to measure the actual rate of electron transfer to the radical cation and the oxyferryl heme in CMPI. Two important design criteria had to be met to achieve this goal. First, the Ru−Cc derivative must interact with CMPI in the same way as native iso-1-Cc. Second, the rate of electron transfer from the photoexcited $Ru^{II*}$ to heme *c* $Fe^{III}$ must be rapid enough to completely resolve the subsequent electron transfer reaction from heme *c* $Fe^{II}$ to the initial acceptor in CMPI. This requires optimum photoredox properties for $Ru^{II*}$ and an efficient pathway for electron transfer from $Ru^{II}$ to the heme group. The single sulfhydryl at Cys-39 on the backside of yeast H39C,C102T iso-1-Cc was labeled with a sulfhydryl-selective tris(bipyridine)ruthenium reagent to form Ru-39-Cc (Geren et al., 1995). Ru-39-Cc satisfies both of the design criteria listed above and was used to measure the rate constants for intracomplex electron transfer to the Trp-191 indolyl radical cation and the oxyferryl heme. Stopped-flow spectroscopy was used to verify that the kinetic mechanism of Ru-39-Cc was the same as that of native yCc under all ionic strength conditions. The location of the binding domain used for reduction of both the radical cation and the oxyferryl heme was determined using a series of surface charge mutants of CcP.

## EXPERIMENTAL PROCEDURES

*Materials*. Yeast iso-1-Ru-39-Cc was prepared as described by Geren et al. (1995). CcP(MI) and the mutants E32Q, D34N, E35N, E290N, E291Q, and A193F were prepared as described (Fishel et al., 1987; Miller et al., 1994b). The A193C-MBP enzyme was prepared as described by Miller et al. (1996).

*Laser Flash Photolysis Studies*. Laser flash photolysis studies of the reaction between Ru-39-Cc and CMPI were carried out as described by Durham et al. (1989) and Geren et al. (1991, 1995). The excitation flash was provided by either the third harmonic of a Nd:YAG laser with a pulse width of 20 ns and a wavelength of 356 nm or a Phase R Model DL 1400 flash lamp-pumped dye laser producing a 450 nm light flash with $<0.5$ $\mu$s duration. The probe source was a pulsed 75 W xenon arc lamp, and the photomultiplier detector had a response time of 20 ns. For slower reactions in the 10 $\mu$s to 1 s time domain, a 100 W quartz halogen lamp was used as the probe source along with a photodiode detector. The excitation response curve $E(t_j)$ for the laser and detection system was recorded using light scattering from a buffer solution with the optical filters removed. The experimental transients were fit by the convolution function $D(t) = \int E(t_j) i(t - t_j) dt_j$, where $i(t)$ is the theoretical response of the system to an infinitely sharp laser pulse, as described by Durham et al. (1989) and Demas (1983). The sample was placed in a glass semimicrocuvette with a path length of 1 cm. Samples contained 5−20 $\mu$M Ru-39-Cc and 5−20 $\mu$M CcP in 1−5 mM sodium phosphate, pH 7.0, containing 0−300 mM NaCl. The transients for the species $Ru^{II}$, $Ru^{II*}$,

Scheme 2

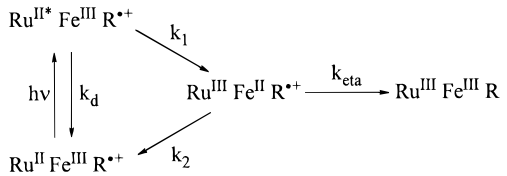


and $Fe^{II}$ in Scheme 2 were detected at the appropriate wavelengths. The $Ru^{II*}$ transient was detected at 556.5 nm, an isobestic point for Cc. The $i(t)$ for Ru(II*) in Scheme 2 is given by

$$i(Ru^{II*})_{556} = \Delta\epsilon_{556} C_o e^{-(k_1+k_d)t} \quad (1)$$

where $\Delta\epsilon_{556} = 1.0\ mM^{-1}\ cm^{-1}$ is the extinction coefficient for $Ru^{II*}$ (Durham et al., 1989) and $C_o$ is the concentration of $Ru^{II*}$ molecules excited in the laser flash. The $Ru^{II*}$ transient was also obtained from the luminescence decay (Durham et al., 1989). The $Fe^{II}$ transient was obtained by subtracting the Ru(II*) transient detected at 556.5 nm from the 550 nm transient, as described by Durham et al. (1989). The $i(t)$ for $Fe^{II}$ is given by

$$i(Fe^{II})_{550} = \Delta\epsilon_{550} C_o A[e^{-(k_1+k_d)t} - e^{-(k_2+k_{eta})t}] \quad (2)$$

where $A = k_1/(k_2 + k_{eta} - k_1 - k_d)$ and $\Delta\epsilon_{550} = 18.6\ mM^{-1}\ cm^{-1}$ is the extinction coefficient for Cc $Fe^{II}$. The $Ru^{II}$ transient was measured at 434 nm, a Cc isobestic:

$$i(Ru^{II})_{434} = \Delta\epsilon_{434} C_o[B - Ce^{-(k_1+k_d)t} + De^{-(k_2+k_{eta})t}] \quad (3)$$

where $\Delta\epsilon_{434} = 9.8\ mM^{-1}\ cm^{-1}$ (Lachish et al., 1979). The parameters *B*, *C*, and *D* are rather complicated functions of the rate constants and are given in the Supporting Information. Under the conditions of the present experiments, *B* ranges from 0.9 to 1.0, *C* from 0.92 to 0.95, and *D* from −0.04 to −0.08. Thus, the 434 nm transient is dominated by the second term in eq 3. The rate constants $k_1$, $k_2$, $k_{et}$, and $k_d$ were determined by optimizing the least-squares fits of the above equations to the transients at all three wavelengths. In the presence of the sacrificial electron donor aniline, $Ru^{III}$ is rapidly reduced and the back reaction represented by $k_2$ is eliminated. Under these conditions, $k_2$ is set to zero in eq 2 and the rate of decay of the $Fe^{II}$ transient is given simply by $k_{eta}$.

*Stopped-Flow Spectroscopy*. The reaction between $yCc^{II}$ and CMPI was studied using a Hi-Tech SF-61 stopped-flow spectrophotometer equipped with a 1 cm flow cell as described by Hahm et al. (1993, 1994) and Miller et al. (1994b). The dead time of the instrument was 2.0 ms. yCc was treated with excess ascorbate and dithiothreitiol to reduce the heme and any disulfide cross-linked dimers, passed through a 1 × 30 cm Bio-Gel P-2 column equilibrated with 2 mM sodium phosphate, pH 7.0, and 50 mM NaCl to remove excess reagent, and stored under nitrogen. Slightly less than 1 equiv of $H_2O_2$ was added to CcP, and the visible spectrum was recorded on a Hewlett-Packard HP8452 spectrophotometer to measure the formation of CMPI. $yCc^{II}$ and CMPI in 5 mM sodium phosphate, pH 7.0, and NaCl were placed in the two syringes of the stopped-flow apparatus, and transients were recorded within 1 min of CMPI formation. Solutions were then removed from the syringes and visible spectra were recorded to determine that $yCc^{II}$ and CMPI remained stable. The transients were fitted to the complete second-order equation

$$\Delta A = \Delta\epsilon\left(b_o - \frac{e^{(b_o-a_o)kt} - 1}{(e^{(b_o-a_o)kt}/a_o - 1/b_o}\right) \quad (4)$$

where $a_o$ is the initial concentration of the excess reactant, $b_o$ is the initial concentration of the limiting reactant, and $\Delta\epsilon$ is the appropriate difference extinction coefficient. For yCc, $\Delta\epsilon_{419} = -44\ mM^{-1}\ cm^{-1}$ and $\Delta\epsilon_{434} = 0$ (Margoliash & Frohwirt, 1959). For CMPI($Fe^{IV}$,$R^{\bullet+}$) → CMPII($Fe^{IV}$,R), $\Delta\epsilon_{419} < 1\ mM^{-1}\ cm^{-1}$, $\Delta\epsilon_{434} = +4\ mM^{-1}\ cm^{-1}$; and for CMPII($Fe^{IV}$,R) → CcP($Fe^{III}$,R), $\Delta\epsilon_{419} = -27\ mM^{-1}\ cm^{-1}$, $\Delta\epsilon_{434} = -27\ mM^{-1}\ cm^{-1}$ (Coulson et al., 1971; Ho et al., 1983). The kinetics were studied using two different protocols. In protocol A, $yCc^{II}$ was mixed with excess CMPI to measure the initial electron transfer reaction. Typical concentrations were [$yCc^{II}$] = 0.2−1 μM and [CMPI] = 0.5−3 μM. In protocol B, excess $yCc^{II}$ was mixed with CMPI to measure the complete reduction of CMPI to CcP. Typical concentrations were [$yCc^{II}$] = 1−10 μM, and [CMPI] = 0.2−1.0 μM.

## RESULTS

*Electron Transfer within the 1:1 Complex between Ru-39-Cc and CMPI*. Photoexcitation of 11 μM Ru-39-Cc in 2 mM sodium phosphate, pH 7.0, resulted in electron transfer from $Ru^{II*}$ to Cc heme $Fe^{III}$ with rate constant $k_1$, followed by electron transfer from $Fe^{II}$ to $Ru^{III}$ with rate constant $k_2$ according to Scheme 2 (without $R^{\bullet+}$ and with $k_{eta} = 0$). The transients for the three species $Ru^{II*}$, $Fe^{II}$, and $Ru^{II}$ were measured at the appropriate wavelengths, and quantitatively fitted to the kinetic equations for Scheme 2. The $Ru^{II*}$ transient measured at 556.5 nm, a Cc isobestic, was fitted to eq 1 with $(k_1 + k_d) = (6.5 \pm 0.5) \times 10^6\ s^{-1}$ and $C_o = 4 \pm 0.4$ μM. The $Ru^{II*}$ transient was also detected from the luminescence decay with the same results, $(k_1 + k_d) = (6.7 \pm 0.6) \times 10^6\ s^{-1}$. The $Fe^{II}$ transient obtained at 550 nm was fitted to eq 2 with an increasing exponential with $(k_1 + k_d) = (6.5 \pm 0.7) \times 10^6\ s^{-1}$ and a decreasing exponential with $k_2 = (1.0 \pm 0.1) \times 10^6\ s^{-1}$ (Figure 1A). The value of $k_1$ was measured from the amplitude of the $Fe^{II}$ transient, using the value of $C_o$ obtained from the amplitude of the 556.5 nm $Ru^{II*}$ transient. The same value of $C_o$ was independently measured from the amplitude of the 434 nm $Ru^{II}$ transient and was stable within ±10% over the entire experiment. A unique set of rate constants were required to simultaneously fit the $Ru^{II*}$, $Fe^{II}$, and $Ru^{II}$ transients. The measured values for 10 μM Ru-39-Cc in 2 mM phosphate, pH 7, are $k_1 = (0.5 \pm 0.07) \times 10^6\ s^{-1}$, $k_2 = (1.0 \pm 0.1) \times 10^6\ s^{-1}$, and $k_d = (6.0 \pm 0.7) \times 10^6\ s^{-1}$. These values are independent of protein concentration, consistent with intraprotein electron transfer. The rate constant $k_d$ includes both the natural decay of $Ru^{II*}$ and energy transfer from $Ru^{II*}$ to $Fe^{III}$. Addition of 12.5 μM CcP to 11 μM Ru-39-Cc in 2 mM phosphate, pH 7.0, had no effect on the values of $k_1$, $k_2$, or $k_d$, indicating that formation of a 1:1 complex between the two proteins did not affect electron transfer between Ru(II*) and heme *c* (Figure 1A). When 1 equiv of hydrogen peroxide was added to the complex to form CMPI, a significant increase in the rate of reoxidation of heme *c* $Fe^{II}$ was observed (Figure 1B), consistent with electron transfer

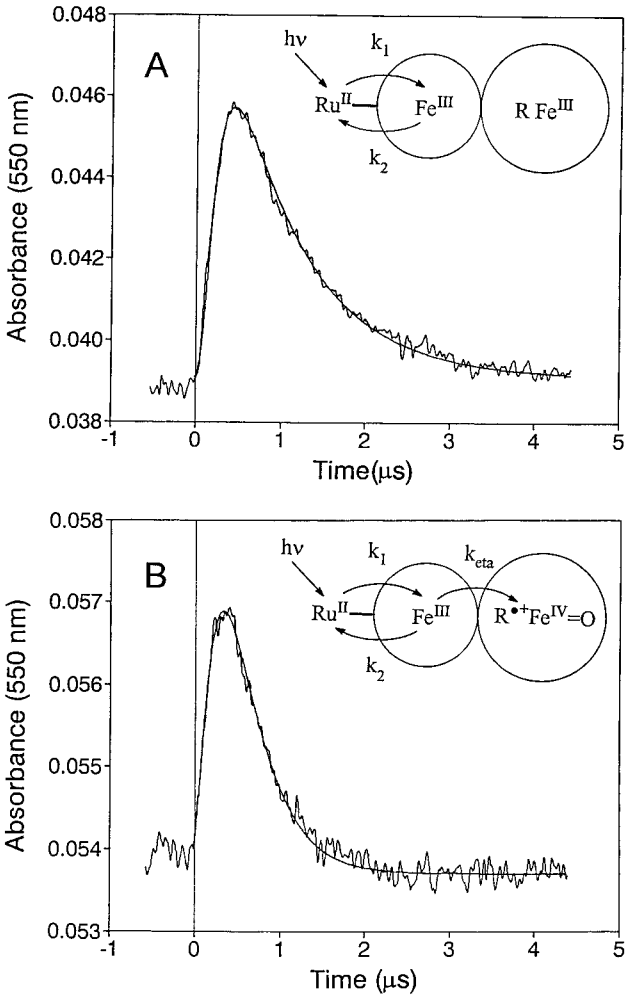


FIGURE 1: Photoinduced electron transfer from Ru-39-Cc$^{II}$ to CMPI. (A) A solution containing 11 $\mu$M Ru-39-Cc and 12.5 $\mu$M CcP in 2 mM sodium phosphate, pH 7.0, was excited with a 450 nm laser flash. The smooth line is the best fit to eq 2 of Scheme 2 with $k_1 = 5.0 \times 10^5$ s$^{-1}$, $k_2 = 1.0 \times 10^6$ s$^{-1}$, and $k_d = 6.0 \times 10^6$ s$^{-1}$. (B) $H_2O_2$ (12.5 $\mu$M) was added to the solution in (A) to form CMPI, and the experiment was repeated. The smooth line is the best fit to eq 2 with $k_1 = 5 \times 10^5$ s$^{-1}$, $k_d = 6 \times 10^6$ s$^{-1}$, and $(k_{eta} + k_2) = 3.0 \times 10^6$ s$^{-1}$. The inset in this and subsequent figures shows the portion of Scheme 2 that is occurring under the conditions used. The rate constant $k_d$ for the decay of Ru$^{II*}$ is not shown in these insets.

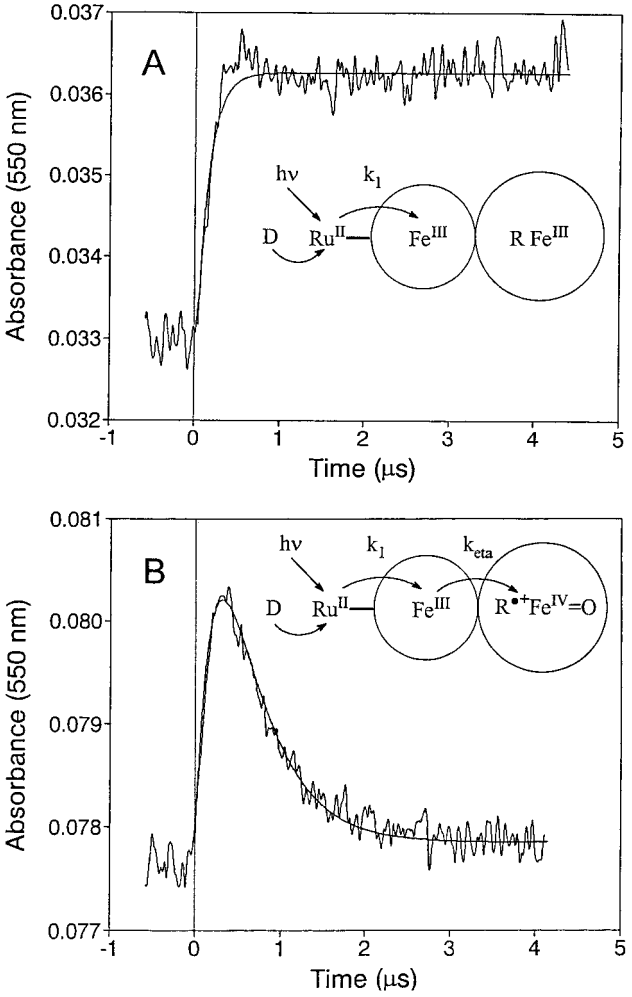


FIGURE 2: Photoinduced electron transfer from Ru-39-Cc$^{II}$ to CMPI in the presence of a sacrificial electron donor. (A) A solution containing 11 $\mu$M Ru-39-Cc and 12.5 $\mu$M CcP in 2 mM sodium phosphate, pH 7.0, and 2 mM aniline was excited with a 450 nm laser flash. The aniline rapidly reduced Ru$^{III}$ and prevented the back electron transfer reaction $k_2$ seen in Figure 1A. The smooth line is the best fit to eq 2 with $(k_1 + k_d) = 6.5 \times 10^6$ s$^{-1}$ and $k_2$ and $k_{eta}$ set to zero. (B) $H_2O_2$ (12.5 $\mu$M) was added to the solution in (A) to form CMPI, and the experiment was repeated. The smooth line is the best fit to eq 2 with $(k_1 + k_d) = 6.5 \times 10^6$ s$^{-1}$ and $k_{eta} = 2.0 \times 10^6$ s$^{-1}$.

to CMPI according to Scheme 2. The Ru$^{II*}$, Fe$^{II}$, and Ru$^{II}$ transients were fitted as described above with $k_1 = (0.5 \pm 0.08) \times 10^6$ s$^{-1}$, $k_d = (6.0 \pm 0.8) \times 10^6$ s$^{-1}$, and $(k_2 + k_{eta}) = (3.0 \pm 0.3) \times 10^6$ s$^{-1}$. It was not possible to separately determine $k_2$ and $k_{eta}$ by this method. However, it is highly unlikely that $k_2$ changes as a result of CMPI formation, since $k_1$ and $k_d$ remain constant. $k_1$ and $k_2$ both represent electron transfer between ruthenium and heme *c* and are expected to change in concert in response to any potential conformational changes (Durham et al., 1989). With the assumption that $k_2$ remains constant at $(1.0 \pm 0.1) \times 10^6$ s$^{-1}$, the rate constant for electron transfer from Fe$^{II}$ to the initial acceptor in CMPI is $k_{eta} = (2.0 \pm 0.3) \times 10^6$ s$^{-1}$.

A different experimental approach was also used to measure intracomplex electron transfer, in which the sacrificial electron donor aniline was present to rapidly reduce Ru$^{III}$ and prevent the back reaction $k_2$. Photoexcitation of a 1:1 complex between Ru-39-Cc and CcP in the presence of aniline resulted in a rapid increase in the absorbance at 550 nm with no subsequent decrease, consistent with Scheme 3.

Scheme 3

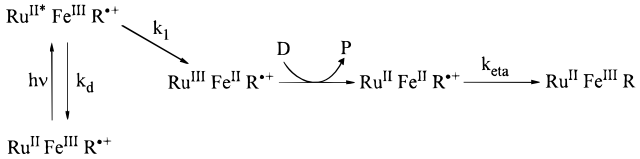


The 550 nm transient is described by eq 2 with $k_2$ and $k_{eta}$ set to zero and thus consists of a single increasing exponential with rate constant $(k_1 + k_d) = (6.5 \pm 0.6) \times 10^6$ s$^{-1}$. When 1 equiv of hydrogen peroxide was added to this sample to form CMPI, the rapid increase in the 550 nm absorbance was followed by an exponential decrease, indicating electron transfer from heme *c* Fe$^{II}$ to the initial acceptor in CMPI (Figure 2B). The 550 nm Fe$^{II}$ transient was fit to eq 2 with $(k_1 + k_d) = (6.5 \pm 0.7) \times 10^6$ s$^{-1}$ and $k_{eta} = (2.0 \pm 0.3) \times 10^6$ s$^{-1}$. The value of $k_{eta}$ is thus the same as in the experiments without aniline. No net decrease in absorbance was observed at 434 nm using either method, indicating that the Trp-191 indolyl radical cation was reduced rather than

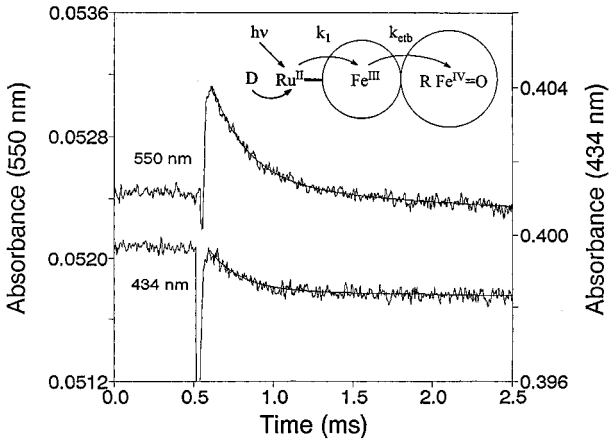


FIGURE 3: Photoinduced electron transfer from Ru-39-Cc$^{II}$ to CMPII. A solution containing 3.3 $\mu$M Ru-39-Cc and 3.4 $\mu$M CMPI in 2 mM sodium phosphate, pH 7.0, and 2 mM aniline was subjected to three laser flashes to completely reduce the Trp-191 radical cation in CMPI to form CMPII as shown in Figure 2B. The next laser flash resulted in the 550 nm transient shown with a rate constant of $k_{etb} = 5000\ s^{-1}$. A transient at 434 nm with the same rate constant indicated reduction of the oxyferryl heme in CMPII.

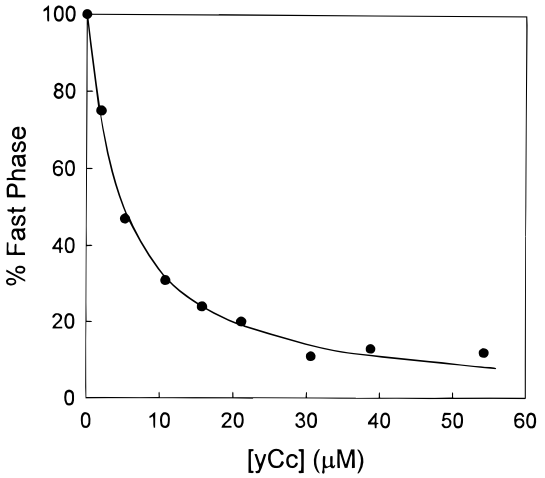


FIGURE 4: Competition between Ru-39-Cc and yCc for the high-affinity binding site on CMPI. Native yCc was added to a solution containing 5 $\mu$M Ru-39-Cc and 5 $\mu$M CMPI in 2 mM sodium phosphate, pH 7, 2 mM aniline, 25 °C, and the amplitude of the fast electron transfer phase due to Ru-39-Cc binding at the high-affinity site was measured. The smooth curve is the fit to the binding equation for the competitive equilibrium, Ru-39-Cc + CMPI $\rightleftarrows$ Ru-39-Cc−CMPI, yCc + CMPI $\rightleftarrows$ yCc−CMPI. The ratio of the dissociation constants for the two complexes was $K_{Ru-39-Cc}/K_{yCc} = 1.05 \pm 0.1$.

the oxyferryl heme (Geren et al., 1991). The radical in CMPI is slowly reduced by aniline (Roe & Goodin, 1993; Hahm et al., 1992). However, under the conditions used here, the half time for this reaction is over 1 order of magnitude larger than the time needed to form CMPI and initiate the laser flash. The measured value of $k_{eta}$ was independent of the concentration of aniline over the range 1−5 mM.

In order to measure the rate of reduction of the oxyferryl heme, a solution containing 5 $\mu$M Ru-39-Cc and 5 $\mu$M CMPI in 2 mM sodium phosphate, pH 7.0, and 1 mM aniline was subjected to a series of laser flashes. Once the radical cation was reduced by the first three flashes as described above, subsequent flashes resulted in a much slower 550 nm transient with a rate constant of $k_{etb} = 5000\ s^{-1}$ (Figure 3). A transient decrease in absorbance with the same rate constant was observed at the Cc isobestic of 434 nm, indicating that this phase represents electron transfer from Ru-39-Cc$^{II}$ to the oxyferryl heme in CMPII(Fe$^{IV}$=O,R). The rate constant $k_{etb}$ for reduction of the oxyferryl heme involves conversion of CMPII(Fe$^{IV}$=O,R) to CMPII(Fe$^{III}$,R$^{\bullet+}$) followed by intracomplex electron transfer from Ru-39-Cc$^{II}$ to R$^{\bullet+}$, as described in the Discussion section. Both $k_{eta}$ and $k_{etb}$ are independent of protein concentration from 5 to 20 $\mu$M in solutions containing CMPI concentrations equal to or greater than that of Ru-39-Cc. When the CMPI concentration was less than that of Ru-39-Cc, an additional very slow phase was observed due to the reaction of solution phase Ru-39-Cc with the 1:1 complex, which will be discussed elsewhere (Mei et al., 1996). These results are consistent with the assignment of $k_{eta}$ and $k_{etb}$ to electron transfer to the radical cation and the oxyferryl heme in 1:1 complexes of Ru-39-Cc with CMPI and CMPII, respectively. The relative dissociation constant of the complex between Ru-39-Cc and CMPI was determined by a competition experiment. Addition of wild-type yCc$^{III}$ to a solution containing 5 $\mu$M Ru-39-Cc and 5 $\mu$M CMPI resulted in a progressive decrease in the amplitude of the fast phase and an increase in the very slow phase (Figure 4). This indicates that wild-type yCc$^{III}$ binds competitively to the same site on CMPI as Ru-39-Cc. Analysis of the data indicated that the ratio of the dissociation constants for Ru-39-Cc and native yCc, $K_d$(Ru-39-Cc)/$K_d$(yCc) was 1.05 ± 0.1 (Figure 4). The absolute value of $K_d$ was too small at 2 mM ionic strength to measure by the ruthenium technique and was estimated to be less than $10^{-7}$ M.

Table 1: Effect of CcP Mutants on Intracomplex Electron Transfer from Ru-39-Cc to the Radical Cation and the Oxyferryl Heme in CMPI[a]

| mutant | $k_{eta}$ ($10^6\ s^{-1}$) | $k_{etb}$ ($10^3\ s^{-1}$) |
|---|---|---|
| CcP(MI) | 2.0 ± 0.3 | 5.0 ± 0.6 |
| E32Q | 2.1 ± 0.3 | 4.3 ± 0.5 |
| D34N | 0.5 ± 0.2 | 1.2 ± 0.2 |
| E35Q | 0.8 ± 0.2 | 2.3 ± 0.3 |
| E290N | 0.9 ± 0.2 | 2.0 ± 0.3 |
| E291Q | 2.0 ± 0.3 | 4.4 ± 0.6 |
| A193F | 0.8 ± 0.2 | 1.5 ± 0.2 |
| A193C-MPB[b] | 0.013 ± 0.002 | 0.07 ± 0.2 |

[a] $k_{eta}$ and $k_{etb}$ were measured as described in Figures 1−3 in 2 mM sodium phosphate, pH 7.0, 22 °C. The error limits were determined from at least three independent measurements. [b] Measured by Miller et al. (1996).

In order to investigate the binding domain used by Cc for reduction of the radical cation and the oxyferryl heme, the effect of CcP surface mutations on $k_{eta}$ and $k_{etb}$ were measured. $k_{eta}$ was decreased 4-fold and 2-fold by the surface charge mutations D34N and E290N, respectively, but was not affected by the mutations E32Q and E291Q (Table 1). Mutation of Ala-193 at the center of the binding domain to a phenylalanine resulted in a 2.5-fold decrease in $k_{eta}$. The effects of the surface mutants on the rate constant $k_{etb}$ for reduction of the oxyferryl heme were approximately the same as the effects on $k_{eta}$ for reduction of the Trp-191 radical cation.

*Effect of Ionic Strength on the Reaction between Ru-39-Cc and CMPI.* The kinetics of the reaction between Ru-39-Cc and CMPI remained nearly the same from 2 mM up to 100 mM ionic strength, where $k_{eta} = (1.2 \pm 0.3) \times 10^6\ s^{-1}$ and $k_{etb} = 3500 \pm 600\ s^{-1}$. A minor slow phase appeared

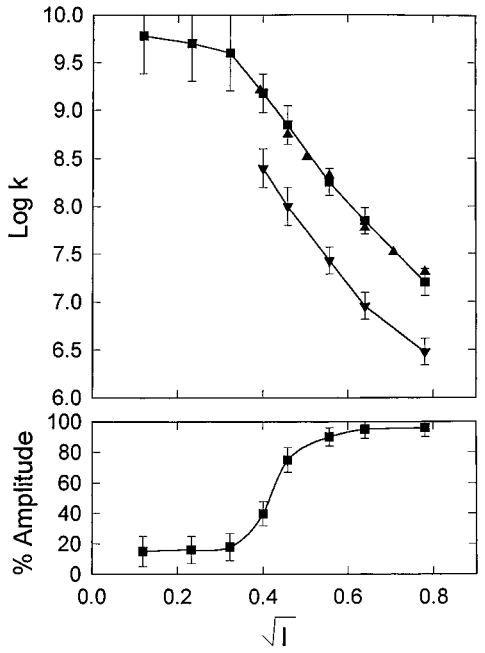


FIGURE 5: Second-order rate constants for the reaction of Ru-39-$Cc^{II}$ and $yCc^{II}$ with CMPI. Top panel: (▲) The second-order rate constant $k_a$ for the reaction of Ru-39-$Cc^{II}$ with the radical cation in CMPI was measured in 5 mM sodium phosphate, pH 7.0, 2 mM aniline, and 150−600 mM NaCl at 22 °C using the ruthenium photoreduction technique as described in the text. (■) The second-order rate constant $k_a$ for the reaction of native $yCc^{II}$ with the radical cation in CMPI was measured using stopped-flow protocol A in 5 mM sodium phosphate, pH 7, and 10−600 mM NaCl at 22 °C. (▼) The second-order rate constant $k_b$ for the reaction of $yCc^{II}$ with the oxyferryl heme in CMPII was measured using stopped-flow protocol B. Bottom panel: Amplitude of the stopped-flow transient for reduction of the radical cation in CMPI as a percentage of the theoretical amplitude for the complete reaction. Protocol A was used with [$yCc^{II}$] = 0.4 $\mu$M and [CMPI] = 0.6 $\mu$M.

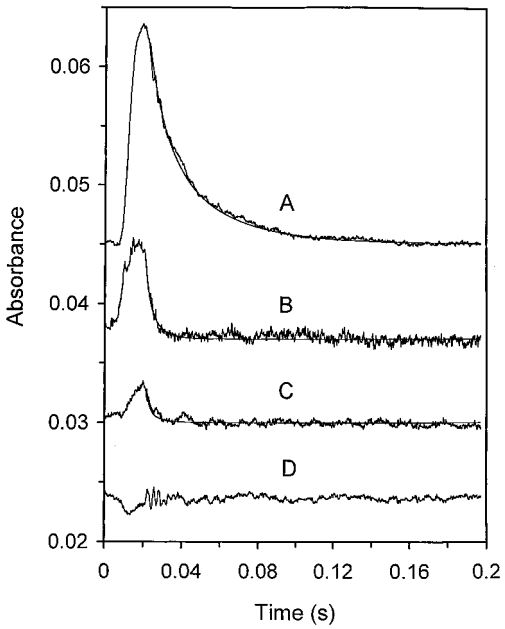


FIGURE 6: Reaction between $yCc^{II}$ and the radical cation in CMPI measured by stopped-flow spectroscopy. The reaction between 0.4 $\mu$M $yCc^{II}$ and 0.6 $\mu$M CMPI was carried out in 5 mM sodium phosphate, 10−300 mM NaCl, pH 7.0, at 22 °C using protocol A: (A) 419 nm transient at 310 mM ionic strength. The smooth line is the best fit to eq 4 with $k_a = 1.7 \times 10^8$ $M^{-1}$ $s^{-1}$ and an observed amplitude of 90% of the theoretical amplitude. (B) 419 nm transient at 160 mM ionic strength, with $k_a = 1.5 \times 10^9$ $M^{-1}$ $s^{-1}$ and an amplitude of 40%. (C) 419 nm transient at 30 mM ionic strength, with $k_a = 7 \times 10^9$ $M^{-1}$ $s^{-1}$ and an amplitude of 15%. (D) 434 nm transient under the same conditions as (C). No 434 nm transient absorbance change was observed at any of the ionic strengths. The transient recording starts before the stopped-flow trigger to show the mixing phase as well as the reaction phase.

in the kinetics at 100 mM ionic strength in addition to the major fast phase due to intracomplex electron transfer to the radical cation. As the ionic strength was increased above 100 mM, the amplitude of the fast phase decreased while the amplitude of the slow phase increased, consistent with complex dissociation. No fast phase was observed at ionic strengths of 200 mM and above. The slow phase had second-order kinetics and was assigned to the bimolecular reaction between solution Ru-39-$Cc^{II}$ and the radical cation in CMPI. The second-order rate constant $k_a$ decreased with increasing ionic strength, reaching a value of $(2.0 \pm 0.4) \times 10^7$ $M^{-1}$ $s^{-1}$ at 610 mM ionic strength (Figure 5). The value of $k_a$ for Ru-39-Cc was that same as that of wild-type yCc from 160 to 610 mM ionic strength (Figure 5). Ru-39-Cc reacted initially with the Trp-191 radical cation in CMPI under all conditions of ionic strength.

*Stopped-Flow Studies of the Reaction between $yCc^{II}$ and CMPI*. The reaction between native $yCc^{II}$ and CMPI was studied using the stopped-flow protocols developed by Hahm et al. (1993, 1994). To measure the initial electron transfer step in the reaction without complications from the second step, $yCc^{II}$ was mixed with excess CMPI according to protocol A. Because of the large rate constant of the initial reaction, it was not generally possible to use a >10-fold excess of CMPI over $yCc^{II}$ to satisfy pseudo-first-order kinetics. The signal-to-noise ratio of the stopped-flow spectrophotometer limited the minimum concentration of $yCc^{II}$ to about 0.2 $\mu$M, while the 2 ms dead time limited the maximum pseudo-first-order rate constant to 350 $s^{-1}$ for detection of at least 50% of the total absorbance change. In view of the complexity of the reaction, it was judged desirable to use a lower excess of CMPI in order to maximize the percentage of the total absorbance change detected. The transients were fitted to the complete second-order eq 4 to measure the rate constant $k_a$. Figure 6A shows the 419 nm transient of the reaction between 0.38 $\mu$M $yCc^{II}$ and 0.60 $\mu$M CMPI in 5 mM sodium phosphate, pH 7.0, 300 mM NaCl, at 22 °C. The second-order rate constant is $(1.7 \pm 0.5) \times 10^8$ $M^{-1}$ $s^{-1}$, and the amplitude of the transient accounted for 90% of the theoretical absorbance change. No absorbance change was observed at 434 nm (a Cc isobestic), indicating that no reduction of the oxyferryl $Fe^{IV}$═O center occurred under these conditions. Experiments with CMPI concentrations ranging from 0.5 to 2 $\mu$M confirmed that the reaction was second order, with a rate constant of $(1.8 \pm 0.5) \times 10^8$ $M^{-1}$ $s^{-1}$ (Table 2). The value of $k_a$ increased continuously as the ionic strength was decreased, until the reaction became too fast to resolve completely in the stopped-flow spectrometer (Figure 5). At 160 mM ionic strength, only 40% of the theoretical amplitude was resolved for the reaction between 0.4 $\mu$M $yCc^{II}$ and 0.6 $\mu$M CMPI with $k_a = (1.5 \pm 0.5) \times 10^9$ $M^{-1}$ $s^{-1}$ (Figure 6B). Even less of the amplitude was resolved at higher CMPI concentrations. At ionic strengths of 100 mM and below, less than 20% of the theoretical amplitude for the reaction between 0.4 $\mu$M $yCc^{II}$ and 0.6 $\mu$M CMPI was resolved (Figures 5 and 6). Under these conditions, it was not possible to measure a value for $k_a$, but only a lower limit of $3 \times 10^9$ $M^{-1}$ $s^{-1}$. No 434 nm

Table 2: Reaction between $yCc^{II}$ and CMPI Measured by Stopped-Flow Spectroscopy[a]

| [$yCc^{II}$] | [CMPI] | % *A* | $k_a$ ($10^8$ $M^{-1}$ $s^{-1}$) |
|---|---|---|---|
| 0.35 | 0.5 | 90 ± 6 | 1.7 ± 0.3 |
| 0.30 | 1.0 | 74 ± 6 | 1.8 ± 0.4 |
| 0.30 | 1.4 | 56 ± 6 | 1.9 ± 0.4 |
| 0.30 | 2.1 | 46 ± 7 | 2.0 ± 0.4 |
| 0.15 | 1.5 | 54 ± 6 | 1.8 ± 0.4 |

[a] The reaction between $yCcI^{II}$ and excess CMPI was measured in 5 mM sodium phosphate, pH 7.0, 300 mM NaCl at 22 °C using protocol A. The second-order rate constant $k_a$ was measured by fitting the 419 nm transient with eq 4. % *A* gives the amplitude of the transient relative to the theoretical amplitude.

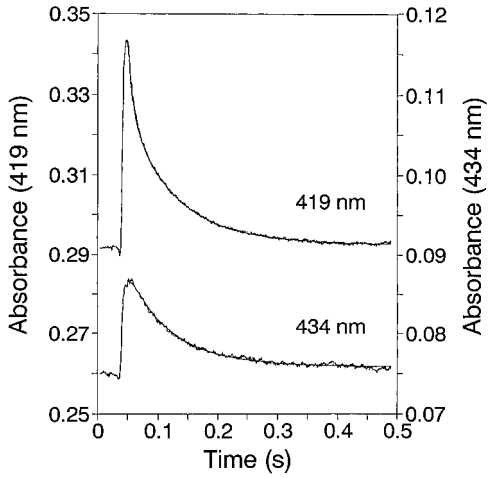


FIGURE 7: Reaction between excess $yCc^{II}$ and CMPI using protocol B. The reaction between 2.4 $\mu$M $yCc^{II}$ and 0.4 $\mu$M CMPI was carried out in 5 mM phosphate, pH 7.0, and 400 mM NaCl at 22 °C and measured at 419 and 434 nm. The smooth lines for both transients show the best fit to Scheme 1 with $k_a = (7.0 \pm 1.0) \times 10^7$ $M^{-1}$ $s^{-1}$ and $K = 0.15 \pm 0.03$ using numerical integration methods. The fast phase of the 419 nm transient was also fit to eq 4 with $k_a = (7.0 \pm 1.0) \times 10^7$ $M^{-1}$ $s^{-1}$. The slow phase in the 419 and 434 nm transients was fit to eq 4 with $k_b = (9.0 \pm 1.5) \times 10^6$ $M^{-1}$ $s^{-1}$.

transient absorbance change was observed at any ionic strength (Figure 6), indicating that the radical cation was the initial electron acceptor. No slower transients were observed at either 416 or 434 nm out to more than 2 min.

To measure both electron transfer steps in the complete reduction of CMPI, excess $yCc^{II}$ was mixed with CMPI according to protocol B. The two phases of reduction were observed most clearly at high ionic strength, where both reactions are slow enough to completely resolve in the stopped-flow spectrometer. The fast phase of the 419 nm transient for the reaction between 2.5 $\mu$M $yCc^{II}$ and 0.4 $\mu$M CMPI at 410 mM ionic strength is due to reduction of the radical in CMPI($Fe^{IV}$=O,$R^{\bullet+}$) with rate constant $k_a = (7.0 \pm 1.0) \times 10^7$ $M^{-1}$ $s^{-1}$ (Figure 7A), the same as measured using protocol A. The slow phase in the 419 nm transient is due to reduction of the oxyferryl heme in CMPII-($Fe^{IV}$=O,R) by a second molecule of $yCc^{II}$ with rate constant $k_b = (9.0 \pm 1.5) \times 10^6$ $M^{-1}$ $s^{-1}$. The 434 nm transient consists of a lag phase due to reduction of the radical cation, followed by a slow phase due to reduction of the oxyferryl heme with the same rate constant $k_b$ measured from the 419 nm transient (Figure 7B). Experiments with $yCc^{II}$ concentrations from 1 to 10 $\mu$M confirmed that both phases obey second-order kinetics. The complete time courses of both the 419 and 434 nm transients were also fitted by Scheme 1

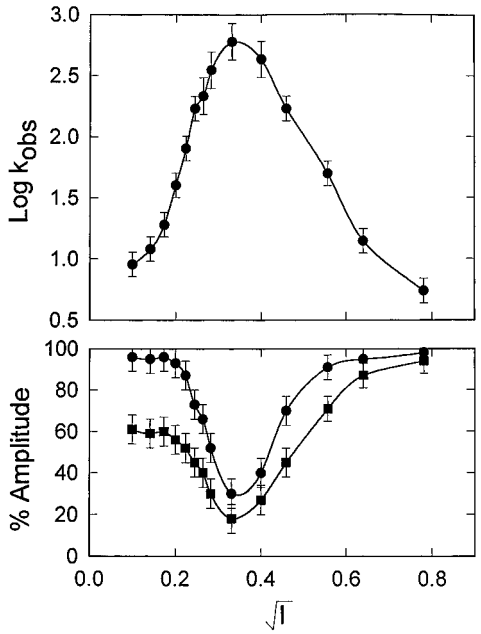


FIGURE 8: Rate constant for the reaction of $yCc^{II}$ with the oxyferryl heme in CMPII. Top panel: The pseudo-first-order rate constant $k_{obs}$ of the slow phase of the 419 and 434 nm transients was measured for the reaction between 2.2 $\mu$M $yCc^{II}$ and 0.4 $\mu$M CMPI in 5 mM sodium phosphate, pH 7, and 0−600 mM NaCl at 22 °C using stopped-flow protocol B. Bottom panel: Amplitudes of the 419 (■) and 434 nm (●) transients as a percentage of the theoretical amplitudes for the complete reaction.

using numerical integration techniques, with $k_a = (7.0 \pm 1.0) \times 10^7$ $M^{-1}$ $s^{-1}$ and $K = 0.15 \pm 0.03$ (Figure 7). In this scheme the observed second-order rate constant for reduction of the oxyferryl heme is given by $k_b = k_a K/(1 + K)$, and it is assumed that the equilibrium between the two forms of CMPII is rapid compared to the bimolecular reactions. The value of $k_b$ is 13% of the value of $k_a$, consistent with $K = 0.15$. Note that reduction of CMPI($Fe^{IV}$=O,$R^{\bullet+}$) to CMPII-($Fe^{IV}$=O,R) is accompanied by a slight increase in absorbance at 434 nm, $\Delta\epsilon_{434} \approx +4$ $mM^{-1}$ $cm^{-1}$ (Coulson et al., 1971). This increase is canceled by an absorbance decrease due to the rapid conversion of 13% of CMPII($Fe^{IV}$=O,R) to CMPII($Fe^{III}$,$R^{\bullet+}$) in the second line of Scheme 1, accounting for the lag phase in protocol B and the absence of a 434 nm transient absorbance change in protocol A (Hahm et al., 1994). As the ionic strength was decreased, both $k_a$ and $k_b$ increased in parallel, and *K* remained approximately constant at 0.17 ± 0.04 (Figure 5). The reduction of the radical cation became too fast to resolve using protocol B at 210 mM ionic strength, and only a single phase was observed in both the 419 and 434 nm transients with $k_{obs} = 170 \pm 40$ $s^{-1}$ and $k_b = (1.0 \pm 0.3) \times 10^8$ $M^{-1}$ $s^{-1}$ (Figures 5 and 8). The amplitudes of the 419 and 434 nm transients were 45% and 70% of the theoretical amplitudes, respectively. The value of $k_{obs}$ increased to 600 ± 150 $s^{-1}$ as the ionic strength was decreased to 110 mM, while the amplitudes of the transients decreased further. However, as the ionic strength was decreased below 100 mM, $k_{obs}$ decreased substantially and reached a value of 9 ± 2 $s^{-1}$ at 10 mM ionic strength, with amplitudes of 61% and 95% for the 419 and 434 nm transients, respectively (Figure 8). Thus, protocol A indicates that the reaction between $yCc^{II}$ and the radical cation in CMPI is too fast to measure by stopped-flow spectroscopy at 10 mM ionic strength, with a second-order rate constant greater than $3 \times 10^9$ $M^{-1}$ $s^{-1}$. Protocol B is consistent with

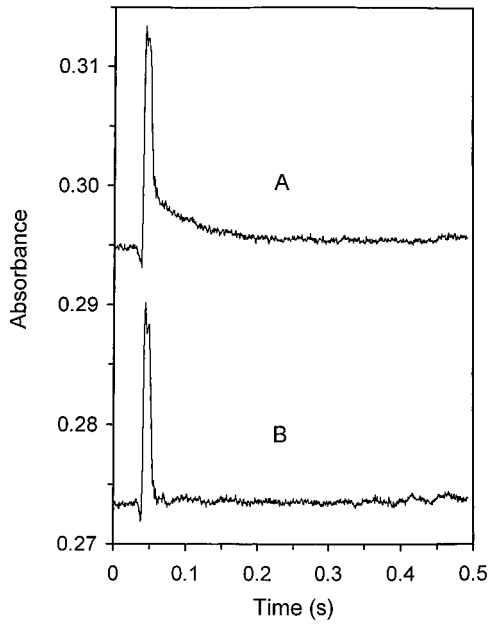


FIGURE 9: Effect of $H_2O_2$ and catalase on the reaction between excess $yCc^{II}$ and CMPI. The reaction between 2.5 $\mu$M $yCc^{II}$ and 0.5 $\mu$M CMPI was measured in 5 mM sodium phosphate, pH 7.0, and 100 mM NaCl at 22 °C and monitored at 419 nm: (A) 0.03 $\mu$M $H_2O_2$ was added to the $yCc^{II}$ solution just before the stopped-flow reaction. The fast phase in the 419 nm transient is due to reduction of the oxyferryl heme in CMPII with $k_{obs} = 600 \pm 150$ $s^{-1}$. The slow phase has $k_s = 23 \pm 4$ $s^{-1}$, and its amplitude of $3.6 \times 10^{-3}$ AU corresponds to the oxidation of 0.08 $\mu$M $yCc^{II}$. In the absence of added $H_2O_2$ the amplitude of this phase is $1.0 \times 10^{-3}$ AU, corresponding to the oxidation of 0.023 $\mu$M $yCc^{II}$. (B) A small amount of C-40 bovine liver catalase from Sigma (10 units/mL, 2 nM) was added to the $yCc^{II}$ solution after addition of $H_2O_2$ as in (A) and incubated for 1 min before stopped-flow mixing. The fast phase due to reduction of the oxyferryl heme was not affected, but the slow phase was completely eliminated.

this result, since only 60% of the theoretical absorbance change was observed in the 419 nm transient. However, the reaction between $yCc^{II}$ and the oxyferryl heme in CMPII-($Fe^{IV}$=O,R) is very slow at 10 mM ionic strength and is nearly completely resolved in the 419 and 434 nm transients. No 419 nm phase due to reduction of the radical cation was resolved below 200 mM ionic strength using protocol B.

An additional slow phase was observed in the 419 nm transients using protocol B with several stock solutions of $yCc^{II}$. This phase was observed most clearly between 50 and 200 mM ionic strength where the reduction of the oxyferryl heme is fast compared to the slow phase. The pseudo-first-order rate constant $k_s$ for this phase was proportional to the total concentration of all forms of CcP, according to the relation $k_s = k_c$[CcP], with $k_c = (4.5 \pm 1.0) \times 10^7$ $M^{-1}$ $s^{-1}$. The rate constant $k_c$ was independent of ionic strength from 50 to 210 mM, and of $yCc^{II}$ concentration from 2 to 10 $\mu$M. The amplitude of this phase was always less than 10% of the amplitude of the major phase due to reduction of the oxyferryl heme, and a corresponding phase was not observed in the 434 nm transient. Since $k_c$ has the same value as the second-order rate constant for the reaction between $H_2O_2$ and CcP, it was postulated that this phase was due to small concentrations of $H_2O_2$ in the $yCc^{II}$ stock solution. The amplitude was increased by addition of a small amount of $H_2O_2$ to the $yCc^{II}$ solution before mixing, without affecting the value of $k_s$ (Figure 9A). This phase was completely eliminated by incubating the $yCc^{II}$ solution with a catalytic concentration of catalase (2 nM) for 1 min prior to the stopped-flow experiment to remove any $H_2O_2$ (Figure 9B). Catalase did not affect the kinetics of reduction of the radical cation or oxyferryl heme. This phase was also eliminated by using fresh $yCc^{II}$ stock solutions that had been passed through a moderately long Biogel P-2 column at 50 mM ionic strength to rigorously remove excess reductant and stored anaerobically until just before addition to the stopped-flow syringe. It is also important to use slightly less than 1 equiv of $H_2O_2$ to oxidize CcP, in order to avoid any excess $H_2O_2$ in the CMPI solution.

## DISCUSSION

*Intracomplex Electron Transfer from Ru-39-$Cc^{II}$ to the Trp-191 Radical Cation in CMPI*. Measurement of the rate constants $k_{eta}$ and $k_{etb}$ for intracomplex electron transfer from yeast cytochrome *c* to the radical cation and the oxyferryl heme in CMPI has been a difficult problem. The ruthenium photoreduction technique has been used to determine that six horse Ru−Cc derivatives labeled at different lysines initially reduced the radical cation in CMPI (Hahm et al., 1993; Liu et al., 1995). The largest intracomplex rate constant was observed for Ru-27-hCc, with $k_{eta} = 6 \times 10^4$ $s^{-1}$. However, the rate constant for yCc is expected to be larger than that for hCc, since there is an additional 7 Å gap between heme *c* and Ala-193 in the electron transfer pathway of the crystalline hCc−CcP complex compared to the yCc−CcP complex (Pelletier & Kraut, 1992). Yeast Ru-102-Cc was found to have a $k_{eta}$ value greater than $5 \times 10^4$ $s^{-1}$ for reduction of the radical cation in CMPI. The reason that only a lower limit could be measured for this derivative is that electron transfer from $Ru^{II*}$ to heme *c* is rate-limiting.

The yeast Ru-39-Cc derivative satisfies both design criteria for measuring intracomplex electron transfer discussed in the introduction. There is an efficient pathway for electron transfer between the ruthenium complex and the heme group which involves 13 covalent bonds and 1 hydrogen bond linking the amide of Gly-41 to the heme propionate (Figure 10). The rate constant for electron transfer from $Ru^{II*}$ to the heme group, $k_1 = 5 \times 10^5$ $s^{-1}$, is close to the maximum for this path, since the driving force of 1.1 eV is close to the reorganization energy of 0.74−1.0 eV (Bjerrum et al. 1995; Fairris et al., 1996). The location of the ruthenium group on the back surface of Ru-39-Cc was designed to allow normal interaction with CcP (Figure 10). The second-order rate constant for the reaction of Ru-39-Cc with the radical in CMPI at ionic strengths from 160 to 610 mM is the same as that for native yCc measured by stopped-flow spectroscopy (Figure 5). In addition, the dissociation constant $K_d$ for the high-affinity complex between Ru-39-Cc and CMPI is the same as for native yCc (Figure 4). These results provide strong evidence for the functional integrity of Ru-39-Cc.

The rate constant $k_{eta}$ for intracomplex electron transfer from Ru-39-Cc to the Trp-191 indolyl radical cation was measured by two different techniques, shown in Figure 1B without a sacrificial donor, and Figure 2B using aniline as a sacrificial donor. The value of $k_{eta}$ was found to be $2.0 \times 10^6$ $s^{-1}$ using either technique and was independent of protein concentration, indicating that it was due to electron transfer within the 1:1 high-affinity complex between the two

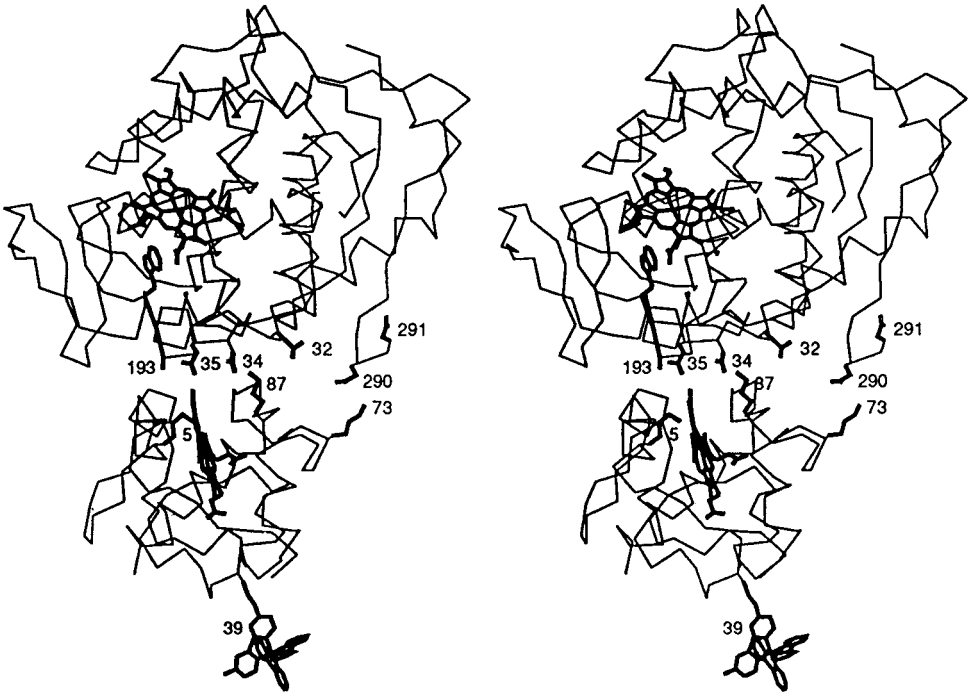


FIGURE 10: X-ray crystal structure of CcP−yCC complex (Pelletier & Kraut, 1992). The ruthenium complex was attached to Cys-39 by molecular modeling. The heme groups of both proteins and the electron transfer pathway consisting of CcP residues Trp-191, Gly-192, Ala-193, and Ala-194 are shown in bold. The side chains of CcP residues E32, D34, E35, D37, A193, E290, and E291 and yCC residues K5, K73, and K87 are shown and labeled.

proteins. The location of the high-affinity interaction domain between yCc and CMPI was investigated using mutants involving CcP surface residues. Mei et al. (1996) found that the charge → amide mutations D34N and E290N increased the equilibrium dissociation constant $K_d$ of the complex between Ru-39-Cc and CMPI by more than 30-fold at low ionic strength. The E35Q mutation had a smaller effect, while the mutations E32Q and E291Q had very little effect. The relative effects of the charge mutations on $K_d$, $k_{eta}$, and $k_{etb}$ parallels the location of these residues at the binding domain of the yCc−CcP crystalline complex (Table 1; Figure 10). Asp-34 and Glu-290 are located within the binding domain with their terminal oxygen atoms 3.8 and 3.2 Å from the amino groups of yCc lysines 87 and 73, respectively (Figure 10). The large increase in $K_d$ due to mutation of these carboxylates to amides could be accompanied by small changes in the orientation of the complex, which could cause the relatively small decreases in $k_{eta}$ (Table 1). Changes of only a fraction of an angstrom in the electron transfer pathway could account for the 2−4-fold decreases in $k_{eta}$. Glu-35 and Glu-32 are located at the edge of the binding domain, with their carboxylate oxygens about 4−5 and 5 Å from the Lys-87 amino group on yCc, respectively (Figure 10). The carboxyl group on Glu-291 projects away from the interface and is 8 Å from the closest lysine on yCc (Figure 10). The small effects of the E32Q and E291Q mutations on $K_d$, $k_{eta}$, and $k_{etb}$ provide an important control for the methodology. The van der Waals interaction between the CcP Ala-193 methyl group and the heme CBC methyl group is at the center of the interaction domain in the crystalline yCc−CcP complex. Addition of a phenyl group to the methyl group of Ala-193 in the A193F mutant results in a 2-fold decrease in $k_{eta}$ (Table 1), consistent with a change in the binding orientation. Substitution of Ala-193 with Cys-193 labeled with the bulky reagent 2-(*N*-maleimidylpropionyl)biocytin (MPB) resulted in a 150-fold decrease in $k_{eta}$ to $1.3 \times 10^4$ $s^{-1}$ (Miller et al., 1996). This modification sterically prevents yCc from binding to the high-affinity binding site with the orientation observed in the crystalline yCc−CcP complex. Instead, yCc can bind in the orientation of the crystalline hCc−CcP complex, which has a 7 Å gap between the edge of heme *c* and the Ala-193 methyl group. The values of $k_{eta}$ for the reaction of the A193C-MBP analogue with horse and yeast Ru−Cc derivatives are comparable (Miller et al., 1996). Previous kinetic and binding studies have indicated that reaction between horse Cc and CMPI utilizes the binding domain of the crystalline hCc−CcP complex (Miller et al., 1994b; Liu et al., 1995; Erman et al., 1996).

The mutagenesis studies discussed above provide evidence that the binding domain identified in the yCc−CcP crystalline complex is used for electron transfer in solution. It is therefore of interest to compare the experimental rate constant $k_{eta}$ with the predictions of several widely used theories for long-range electron transfer utilizing the X-ray crystal structure information. These theories are based on the semiclassical relationship developed by Marcus (Marcus, 1956; Marcus & Sutin, 1985):

$$k_{et} = \frac{4\pi^2}{h} H_{AB}{}^2 \frac{1}{(4\pi\lambda RT)^{1/2}} \exp[-(\Delta G^{\circ\prime} + \lambda)^2/4\lambda RT] \quad (5)$$

$H_{AB}$ describes the electronic coupling between the redox centers, and $\lambda$ is the nuclear reorganization energy. $k_{et}$ assumes its maximum activationless value, $k_{max}$, when the driving force $-\Delta G^{\circ}$ matches the reorganization energy $\lambda$ and the exponential term in eq 5 is equal to 1. Marcus originally suggested that the electronic coupling term can be described approximately by a simple exponential dependence on the

distance between the redox centers:

$$H_{AB}{}^2 = H_o{}^2 \exp(-\beta R) \quad (6)$$

where $R$ is the edge-to-edge distance between the two redox centers and $H_o$ is the maximum electronic coupling. Moser et al. (1992) found that in a broad range of biological systems $k_{max}$ decreases exponentially with the distance $R$, with $\beta = 1.4$ Å$^{-1}$ and an intercept of $10^{13}$ s$^{-1}$ at the van der Waals contact distance of $R = 3.6$ Å. The distance between the closest heme macrocycle atom of yCc and the closest Trp-191 indole ring atom in CcP is 16.0 Å in the crystalline yCc−CcP complex. The maximum, activationless rate constant for this distance using the parameters suggested by Moser et al. (1992) is $k_{max} = 3 \times 10^5$ s$^{-1}$. Beratan and co-workers (1992) developed a dominant pathway model for electron transfer in which the electronic coupling is described by a combination of through-bond, through-hydrogen-bond, and through-space contributions which maximize the overall coupling. The best pathway between heme *c* and the Trp-191 indolyl radical cation in the crystalline yCc−CcP complex consists of two covalent bonds from the heme macrocycle to the heme CBC methyl group, a van der Waals contact of 4.1 Å between the heme CBC methyl group and the Ala-193 methyl group, and nine covalent bonds from the Ala-193 methyl group to the indole group on Trp-191 (Figure 10). Application of the dominant pathway model to this pathway yields a $k_{max}$ value of $2 \times 10^5$ s$^{-1}$, assuming that the hydrogen atoms in the heme CBC and Ala-193 methyl groups are in van der Waals contact with a separation of 2.0 Å. The theoretical value of $k_{et}$ in eq 1 will be less than $k_{max}$ if the driving force $-\Delta G°$ is not equal to the reorganization energy $\lambda$. Unfortunately, neither the driving force nor the reorganization energy of the reaction between heme *c* and the radical cation are known. Mondal et al. (1996) measured a potential of +0.74 V for the two-electron reduction of CMPI using cyclic voltammetry but were not able to determine the individual reduction potentials of the radical cation and oxyferryl heme. Miller et al. (1994b) estimated from stability considerations that the redox potential of the Trp-191 radical cation is about 0.65 V. Using these estimates and a redox potential of 0.25 V for heme *c*, a driving force of $-\Delta G° = 0.4-0.5$ eV can be estimated. The reorganization energy of Cc has been estimated to be about 1.0 eV in solution (Bjerrum et al., 1995; Fairris et al., 1996), but complex formation with CcP is likely to decrease this value (Scott et al., 1994). There is no information on the reorganization energy of the Trp-191 indolyl radical cation, but it is likely to be small since the radical is well-removed from solvent and no changes in bonding are required for reduction. The reorganization energy for electron transfer from yCc$^{II}$ to Trp$^{\bullet+}$ is estimated to be in the range 0.4−0.8 eV, assuming that it is the average of the reorganization energies of the two reactants (Marcus & Sutin, 1985). It thus appears that the driving force is comparable to or less than the reorganization energy, and $k_{et}$ may be somewhat less than $k_{max}$. Therefore, theoretical predictions for $k_{et}$ based on both the distance and pathways models are less than the experimental value of $k_{eta} = 2 \times 10^6$ s$^{-1}$ by a factor of 8 or more. These initial theoretical predictions are necessarily only approximate but serve to point out the complexities of modeling long-range intracomplex electron transfer. This comparison with theory indicates that electron transfer from yCc to the Trp-191 indolyl radical cation in CMPI is very efficient and unlikely to be controlled by conformational gating (Hoffman & Ratner, 1987).

Scheme 4

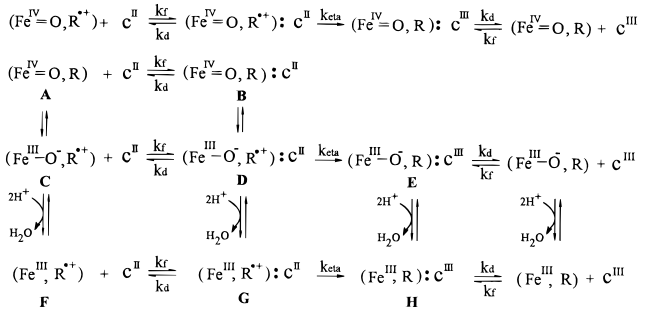


*Mechanism for Electron Transfer from Cc$^{II}$ to the Oxyferryl Heme in CMPII.* The rate constant for intracomplex electron transfer from Ru-39-Cc to the oxyferryl heme in CMPII is $k_{etb} = 5000$ s$^{-1}$. The effects of the surface mutations on $k_{etb}$ were approximately the same as the effects on $k_{eta}$, indicating that the Pelletier−Kraut binding domain and electron transfer pathway are also used for the reduction of the oxyferryl heme in CMPII. The 70-fold decrease in $k_{etb}$ caused by the A193C-MPB substitution supports this conclusion (Table 1) and indicates that no other binding site can significantly contribute to electron transfer to the oxyferryl heme. A mechanism for the complete reduction of CMPI, which includes yCc binding and dissociation as well as proton transfer to and $H_2O$ release from the heme, is shown in Scheme 4. For simplicity, it is assumed that the rate constants $k_f$ and $k_d$ for formation and dissociation of the 1:1 complex do not depend on the redox states of Cc or CcP. (Cc is represented by c in Scheme 4.) The top line of Scheme 4 gives a mechanism for reduction of the Trp-191 radical cation in CMPI by Cc$^{II}$. Complete reduction of the oxyferryl heme in CMPII by solution Cc$^{II}$ involves the steps leading from A to H. Internal electron transfer from Trp-191 to the oxyferryl heme in A results in formation of C, which is postulated to be in rapid equilibrium with A but present in only small concentrations. Proton transfer to the Fe$^{III}$−O$^-$ oxygen in C then results in release of $H_2O$ and formation of F. Coulson et al. (1971) first observed two forms of CMPII, A and F and reported that the equilibrium constant $K = [F]/[A]$ decreased from 1.2 at pH 5.0 to 0.15 at pH 7.0. Ho et al. (1984) found that the rate of conversion of the stable form of A to F is slow but postulated that it is much faster in the conformation of A present immediately following reduction of the radical cation in CMPI. Liu et al. (1994) directly measured the rate constant for the conversion of this conformation of A to F to be 1100 s$^{-1}$ at pH 5.0 and 550 s$^{-1}$ at pH 6.0. They presented evidence that the reduction of the oxyferryl heme by yCc$^{II}$ under stopped-flow conditions at high ionic strength involves the sequence of steps A → C → F → G → H, which is the same as in Scheme 1. The value of $k_b$ is about 14% of the value of $k_a$ at ionic strengths from 160 to 610 mM at pH 7.0 (Figure 5), consistent with $K = [F]/[A] = 0.17 \pm 0.04$. Although it has not been possible to directly measure the rate constant for conversion of A to F at pH 7.0, it is likely to be about 500 s$^{-1}$ (Liu et al., 1994). The $k_{obs}$ for reduction of the oxyferryl heme is smaller than 500 s$^{-1}$ from 160 to 600 mM ionic strength, so the rate of conversion from A to F does not limit the reaction.

Intracomplex electron transfer from bound Ru-39-$Cc^{II}$ to the oxyferryl heme in CMPII involves the steps leading from B to H. The rate constant for this process, $k_{etb} = 5000\ s^{-1}$, is much larger than the rate constant for conversion of B to G, which is assumed to be the same as that for the conversion of A to F. However, this slow step could be bypassed by electron transfer from $yCc^{II}$ to $R^{\bullet+}$ in D to form E, followed by proton transfer and $H_2O$ release to form H. The rate of intracomplex electron transfer to the oxyferryl heme would then be given by $k_{etb} = k_{eta}K_{DB}/(1 + K_{DB})$, where $K_{DB} = [D]/[B]$ and the rate constant for the equilibrium between B and D is assumed to be fast compared to $k_{eta}$. $K_{DB}$ is found to be $2.5 \times 10^{-3}$ at pH 7.0, using $k_{etb} = 5000\ s^{-1}$ and $k_{eta} = 2 \times 10^6\ s^{-1}$. The rate for conversion from D to G is limited by the rate of proton transfer and/or release of $H_2O$ from the heme iron. These processes could be considerably faster in the conversion from E to H than D to G due to the removal of the electrostatic effect of the Trp-191 radical cation. Although intermediates C and D have not been detected directly, several lines of evidence support the requirement for an oxidizable indole at residue 191 for reduction of the oxyferryl heme. First, replacement of Trp-191 with Phe decreases the rate of reduction of the oxyferryl heme by more than $10^4$ (Miller et al., 1995) but leads to only minor changes in the conformation of the proximal heme pocket (Wang et al., 1990). Since the phenyl ring in the mutant is just as close to the heme as the indole ring in CcP(MI), the rate of electron transfer should not have been affected by the mutation if the Trp-191 indole simply acted as a passive conduit. Second, replacement of Met-230 by Ile decreases the rate of reduction of the oxyferryl heme by 10-fold and prevents the formation of intermediate G (Liu et al., 1994). Since the mutation caused virtually no change in the conformation of Trp-191 in the heme pocket, it was postulated that the sulfur atom on Met-230 stabilizes the Trp-191 radical cation and favors formation of intermediates D and G. Both of these results indicate that the oxidation and reduction of Trp-191 plays an essential role in electron transfer from $Cc^{II}$ to the oxyferryl heme. Scheme 4 provides a mechanism for reduction of the oxyferryl heme under a diverse range of conditions. The relative concentrations of the three forms of CMPII at pH 7.0 are [A]:[C]:[F] = [B]:[D]:[G] = 86%:0.25%:14%. Under saturating $yCc^{II}$ conditions, the reaction will follow the pathway B → D → E → H and the intracomplex rate constant $k_{etb}$ will be 0.25% of $k_{eta}$. However, when [$yCc^{II}$] is small and rate-limiting, the reaction will follow the pathway A → C → F → G → H, and the second-order rate constant $k_b$ will be 14% of $k_a$.

*Sequence for Reduction of the Trp-191 Radical Cation and the Oxyferryl Heme in CMPI by $yCc^{II}$.* Coulson et al. (1971) carried out a detailed study of the reaction between horse Cc and CMPI using both visible spectroscopy and ESR spectroscopy to define the products of the reaction. They found that addition of 1 equiv of $hCc^{II}$ to CMPI led to reduction of the radical cation to form CMPII($Fe^{IV}$═O,R) at pH 7 and above, with less than 20% CMPII($Fe^{III}$,$R^{\bullet+}$) formed. In the present studies, the Trp-191 indolyl radical cation in CMPI was found to be the initial site of reduction by yeast Ru-39-$Cc^{II}$ under all conditions of concentration and ionic strength. Yeast Ru-102-Cc as well as six different horse Ru−Cc derivatives have also been found to initially reduce the radical cation in CMPI under all conditions (Geren et al., 1991; Hahm et al., 1993; Liu et al., 1994). Previous stopped-flow studies in our laboratory have demonstrated that the radical cation is the initial reduction site in the reaction with native horse $Cc^{II}$ at all ionic strengths (Hahm et al., 1994), and with native $yCc^{II}$ at ionic strengths from 600 mM down to at least 200 mM (Miller et al., 1994b). In contrast, Matthis et al. (1995) recently reported that the oxyferryl heme is the initial site reduced by $yCc^{II}$ at ionic strengths below 200 mM, while the radical cation is initially reduced at higher ionic strength. Summers and Erman (1988) and Nuevo et al. (1993) also reported that the initial reduction site for horse Cc was the oxyferryl heme at ionic strengths up to 100 mM, and the radical cation at higher ionic strength. The stopped-flow protocol used by Matthis et al. (1995) and Nuevo et al. (1993) involves the use of excess $Cc^{II}$ to fully reduce CMPI to CcP. The mechanism for the reaction under these conditions is very complicated, with two one-electron-reduction reactions each involving complex formation, intracomplex electron transfer, and complex dissociation (e.g., Scheme 4). The rate constant for the reaction is so rapid at ionic strengths below 200 mM that less than 50% of the amplitude is resolved in the stopped-flow spectrometer, further complicating the analysis. In addition, the second low-affinity Cc binding site appears to affect the mechanism at low ionic strength (Matthis et al., 1995; Zhou et al., 1995).

We believe that the key experiment to determine the initial site of reduction in CMPI is protocol A, in which $Cc^{II}$ is mixed with excess CMPI. This protocol ensures that only the initial electron transfer reaction is observed, without complications arising from the second electron transfer reaction or the low-affinity binding site. The reaction detected by protocol A will consist of complex formation between $Cc^{II}$ and CMPI, followed by intracomplex electron transfer to the initial acceptor (the first two steps of the top line of Scheme 4). Experiments using protocol A indicate that $yCc^{II}$ initially reduces the radical cation in CMPI at high ionic strength, as generally agreed (Figure 6). The second-order rate constant $k_a$ for this reaction increases uniformly as the ionic strength is decreased, until it becomes too fast to resolve in the stopped-flow spectrophotometer (Figures 5 and 6). At ionic strengths below 120 mM, less than 20% of the reaction was resolved, and the second-order rate constant $k_a$ was estimated to be larger than $3 \times 10^9\ M^{-1}\ s^{-1}$. No absorbance change was detected at 434 nm at times from 2 ms to several minutes, indicating no reduction of the oxyferryl heme. The final product of the reaction is therefore CMPII($Fe^{IV}$═O,R), in agreement with the equilibrium titration studies of Coulson et al. (1971). The ionic strength dependence of the bimolecular reaction between $yCc^{II}$ and CMPI is the same as for Ru-39-Cc, measured using the ruthenium photoreduction technique (Figure 5). This ionic strength dependence is consistent with a bimolecular reaction between oppositely charged proteins (Smith et al., 1981). It is concluded that $yCc^{II}$ binds to CMPI with a second-order rate constant $k_f$ that is close to the diffusion limit at low ionic strength, followed by rapid intracomplex electron transfer to the Trp-191 indolyl radical cation (Scheme 4).

Protocol B was used to study both electron transfer reactions by mixing excess $yCc^{II}$ with CMPI. The reaction between 2.5 $\mu$M $yCc^{II}$ and 0.4 $\mu$M CMPI at 410 mM ionic strength proceeded in two phases corresponding to the initial reduction of the radical in CMPI with rate constant $k_a = (7.0 \pm 1.0) \times 10^7\ M^{-1}\ s^{-1}$, followed by reduction of the oxyferryl heme in CMPII with rate constant $k_b = (9.0 \pm$

1.5) $\times$ $10^6$ $s^{-1}$. When the ionic strength was decreased, both second-order rate constants $k_a$ and $k_b$ increased in parallel (Figure 5) and reached a point where neither reaction could be completely resolved in the stopped-flow spectrophotometer. The initial reduction of the radical cation could not be resolved at ionic strengths below 220 mM. At the higher $Cc^{II}$ concentrations used in protocol B (e.g., 2.5 $\mu$M), the reduction of the radical cation would occur with a $k_{obs}$ value of about $k_a \times 2.5\ \mu M = 1250\ s^{-1}$ at 210 mM ionic strength, and only 8% of the reaction would be resolved in the stopped-flow spectrometer with a dead time of 2 ms. Less than 1% of the reaction would be resolved at ionic strengths below 120 mM. The rate constant $k_{obs}$ for reduction of the oxyferryl heme was very large at ionic strengths between 100 and 200 mM, and less than 50% of the reduction of the oxyferryl heme was resolved (Figure 8). However, the rate constant decreased below 100 mM ionic strength, and a single slow phase was observed in both the 416 and 434 nm transients at 10 mM ionic strength with $k_{obs} = 10\ s^{-1}$. The amplitudes of the 416 and 434 nm transients were close to the theoretical values for reduction of the oxyferryl heme, with no additional phase that could be assigned to reduction of the radical cation. Protocols A and B indicate that at low ionic strength $yCc^{II}$ initially reduces the radical cation in CMPI in a bimolecular reaction that is close to the diffusion limit. A second molecule of $yCc^{II}$ then reduces the oxyferryl heme in CMPII with a very small rate constant. Since $k_{obs}$ is much smaller than the rate constant $k_{etb}$ for intracomplex electron transfer to the oxyferryl heme, it is concluded that the rate-limiting step is dissociation of $yCc^{III}$ from the CMPII-($Fe^{IV}$,R)$-yCc^{III}$ product complex before the second molecule of $yCc^{II}$ can bind (Scheme 4). The product dissociation rate constant $k_d$ is expected to increase with increasing ionic strength, accounting for the 60-fold increase in $k_{obs}$ as the ionic strength is increased from 10 to 100 mM (Figure 8). The direct measurement of $k_d$ over a wide range of ionic strength was described by Mei et al. (1996) and Miller (1996). $yCc^{II}$ also binds to a second low-affinity site on CcP at low ionic strength and affects the kinetic mechanism (Zhou et al., 1995; Matthis et al., 1995). Mei et al. (1996) and Miller (1996) presented evidence that $yCc^{II}$ binding at the low-affinity site increases the rate constant $k_d$ for dissociation of $yCc^{III}$ from the high-affinity binding site, thus increasing the overall rate of reduction of the oxyferryl heme. They did not find evidence for direct electron transfer from $yCc^{II}$ in the low-affinity binding site to either the Trp-191 radical cation or oxyferryl heme.

The experimental conditions used by Matthis et al. (1995) are essentially the same as protocol B, and our results for reduction of the oxyferryl heme are in general agreement with theirs. At a concentration of 1 $\mu$M $yCc^{II}$ and 0.2 $\mu$M CMPI, they observed an increase in $k_{obs}$ for reduction of the oxyferryl heme as the ionic strength was decreased from 300 to 100 mM, followed by a substantial decrease at lower ionic strength. They did not observe the rapid reduction of the radical cation at ionic strengths below 200 mM, which is in agreement with our results showing that this reaction is too fast to resolve using protocol B.

Matthis et al. (1995) reported an additional very slow phase at ionic strengths below 200 mM which was attributed to reduction of the radical cation in CMPII($Fe^{III}$,$R^{\bullet+}$). We have also observed a slow phase with the same kinetic properties as reported by Matthis et al. (1995). However, evidence is presented that this phase was due to a small concentration of $H_2O_2$ that occurred in several stock solutions of $yCc^{II}$. Addition of a small amount of $H_2O_2$ to the $yCc^{II}$ solution resulted in an increase in the amplitude of the slow phase with no change in the rate constant. Most significantly, the slow phase was completely eliminated by incubation of the $yCc^{II}$ solution with catalase, which specifically converts $H_2O_2$ to $H_2O$ and $O_2$. All of the kinetic properties reported in the present studies and by Matthis et al. (1995) are consistent with the interpretation that this phase is due to enzyme turnover by a small concentration of $H_2O_2$ in the $yCc^{II}$ solution according to eq 7. This phase is only observed

$$\mathrm{CcP} + \mathrm{H_2O_2} \xrightarrow{k_p} \mathrm{CMPI};\qquad \mathrm{CMPI} + 2\mathrm{yCc^{II}} \xrightarrow{\text{fast}} \mathrm{CcP} + 2\mathrm{yCc^{III}} \quad (7)$$

under conditions where it is slow compared to the reduction of the radical cation and oxyferryl heme by $yCc^{II}$ (i.e., below 200 mM ionic strength). Therefore, the CMPI present at the beginning of the stopped-flow experiment will have been converted to CcP before this phase begins. Since the second step in eq 7 is fast compared to the first step, the pseudo-first-order rate constant $k_s$ will be independent of the concentration of $yCc^{II}$, as observed. No transient absorbance change will be observed at 434 nm for this phase since CMPI is reduced much faster than it is formed and does not build up. The second-order rate constant for the reaction between CcP and $H_2O_2$ is $k_p = 4.6 \times 10^7\ M^{-1}\ s^{-1}$ (Vitello et al., 1990), and since [$H_2O_2$] is smaller than [CcP] under the conditions examined, the pseudo-first-order rate constant will be $k_s \approx k_p$[CcP]. The same kinetic equation is observed for the slow phase, $k_s = k_c$[CcP], and the values of $k_c$ reported by Matthis et al. (1995), $(5.2 \pm 0.2) \times 10^7\ M^{-1}\ s^{-1}$, and in the present studies, $(4.5 \pm 1.0) \times 10^7\ M^{-1}\ s^{-1}$, are essentially the same as $k_p$. Furthermore, $k_c$ and $k_p$ are both independent of ionic strength (Matthis et al., 1995; Vitello et al., 1990). A slow phase with the same kinetic properties was also observed during the reduction of CMPI by excess horse $Cc^{II}$ at ionic strengths below 100 mM, with $k_c = (4.0 \pm 2.5) \times 10^7\ M^{-1}\ s^{-1}$ (Summers & Erman, 1988; Nuevo et al., 1993). Although it is uncertain how $H_2O_2$ could be formed in the $yCc^{II}$ solution, it is known that both $hCc^{II}$ and $yCc^{II}$ are slowly autoxidized in the presence of $O_2$. It is postulated that small concentrations of $H_2O_2$ and other oxidized species could build up during this autoxidation. An $H_2O_2$ concentration of less than 3% of the $yCc^{II}$ concentration would account for the slow phase observed in the present studies and in Figure 1 of Matthis et al. (1995). With this explanation for the slow phase, the data of Matthis et al. (1995), Neuvo et al. (1993), and Summers and Erman (1988) are consistent with a mechanism in which both $yCc^{II}$ and $hCc^{II}$ first reduce the Trp-191 radical cation in CMPI and then the oxyferryl heme in CMPII at all ionic strengths.

Pappa et al. (1996) recently prepared two specifically cross-linked yCc$-$CcP complexes. Complex 2 was designed to mimic the Pelletier$-$Kraut crystalline complex, while complex 3 is cross-linked at CcP residue 149 on the opposite side of the molecule. In both complexes, the cross-linked $yCc^{II}$ was found to transfer an electron to the Trp-191 radical cation in CMPI rather than the oxyferryl heme. The rate constant for electron transfer in complex 2 was too fast to measure by stopped-flow spectroscopy and was estimated

to be greater than 800 $s^{-1}$. The rate constant was much smaller in complex 3, about 1 $s^{-1}$. Electron transfer from $yCc^{II}$ to the Trp-191 radical in complex 3 was unexpected because heme *c* is closer to the oxyferryl heme than to Trp-191, 14−18 Å versus 20−23 Å. In addition, small molecules such as aniline first reduce the radical in CMPI (Roe & Goodin, 1993), even though they appear to react near the *δ*-meso edge of the heme on the opposite side from Trp-191 (Wilcox et al., 1996). These results suggest that the Trp-191 radical cation is the initial site of reduction in CMPI *regardless* of the pathway for electron transfer. Trp-191 is in van der Waals contact with the CcP heme, and the oxyferryl heme and radical cation are coupled by weak spin exchange (Huyett et al., 1995). Reduction of the radical cation is thermodynamically favored at pH 7 or greater (Coulson et al., 1971) and also kinetically favored because of the large reorganization energy for reduction of the oxyferryl heme due to the need for proton transfer and $H_2O$ release (Roe & Goodin, 1993). Rapid electron transfer between the Trp-191 indole and the oxyferryl heme (such as proposed between A and C in Scheme 4) would ensure that the radical is reduced first regardless of the source of the electron. It therefore appears that reduction of both the radical cation and the oxyferryl heme in CMPI involves a high degree of coupling between the two redox centers.

## ACKNOWLEDGMENT

We thank Dr. Joseph Kraut for enlightening discussions on the structure and mechanism of CcP.

## SUPPORTING INFORMATION AVAILABLE

Parameters *B*, *C*, and *D* for Scheme 2 (1 page). Ordering information is given on any current masthead page.

## REFERENCES

Beratan, D. N., Betts, J. N., & Onuchic, J. N. (1992) *J. Chem. Phys. 96*, 2852−2855.

Bjerrum, M. J., Casimioro, D. R., Chang, I.-J., D Bilio, A. J., Gray, H. B., Hill, M. G., Langen, R., Mines, G. A., Skov, L. K., Winkler, J. R., & Wuttke, D. S. (1995) *J. Bioenerg. Biomembr. 27*, 295−303.

Coulson, A. F. W., Erman, J. E., & Yonetani, T. (1971) *J. Biol. Chem. 246*, 917−924.

Durham, B., Pan, L. P., Long, J., & Millett, F. (1989) *Biochemistry 28*, 8659−8665.

Erman, J. E., Vitello, L. B., Mauro, J. M., & Kraut, J. (1989) *Biochemistry 28*, 7992−7995.

Erman, J. E., Krescheck, G. C., Vitello, L. B., & Miller, M. A. (1996) (to be submitted).

Fairris, J. L., Wang, K., Geren, L., Saunders, A. J., Pielak, G. J., Durham, B., & Millett, F. (1996) Advances in Chemistry Series (in press).

Fishel, L. A., Villafranca, J. E., Mauro, J. M., & Kraut, J. (1987) *Biochemistry 26*, 351−360.

Fitzgerald, M. M., Churchill, M. J., McRee, D. E., & Goodin, D. B. (1994) *Biochemistry 33*, 3807−3818.

Geren, L. M., Hahm, S., Durham, B., & Millett, F. (1991) *Biochemistry 30* 9450−9457.

Geren, L. M., Beasley, J. R., Fine, B. R., Saunders, A., Hibdon, S., Pielak, G. J., Durham, B., & Millett, F. (1995) *J. Biol. Chem. 270*, 2466−2472.

Goodin, D. B., & McRee, D. E. (1993) *Biochemistry 32*, 3313−3324.

Hahm, S., Durham, B., & Millett, F. (1992) *Biochemistry 31*, 3472−3477.

Hahm, S., Geren, L., Durham, B., & Millett, F. (1993) *J. Am. Chem. Soc. 115*, 3372−3373.

Hahm, S., Miller, M. A., Geren, L., Kraut, J., Durham, B., & Millett, F. (1994) *Biochemistry 33*, 1473−1480.

Hazzard, J. T., & Tollin, G. (1991) *J. Am. Chem. Soc. 113*, 8956−8957.

Hazzard, J. T., Poulos, T., & Tollin, G. (1987) *Biochemistry 26*, 2836−2848.

Heacock, D., Liu, R., Yu, C., Yu, L., Durham, B., & Millett, F. (1993) *J. Biol. Chem. 268*, 27171−27175.

Ho, P. S., Hoffman, B. M., Kang, C. H., & Margoliash, E. (1983) *J. Biol. Chem. 258*, 4356−4363.

Hoffman, B. M., & Ratner, M. A. (1987) *J. Am. Chem. Soc. 109*, 6237−6243.

Huyett, J. E., Doan, P. E., Gurbiel, R., Houseman, A. L. P., Sivaraja, M., Goodin, D. B., & Hoffman, B. M. (1995) *J. Am. Chem. Soc. 117*, 9033−9041.

Liu, R.-Q., Hahm, S., Miller, M. A., Han, G. W., Geren, L., Hibdon, S., Kraut, J., Durham, B., & Millett, F. (1994) *Biochemistry 33*, 8678−8685.

Liu, R., Hahm, S., Miller, M., Durham, B., & Millett, F. (1995) *Biochemistry 34*, 973−983.

Marcus, R. A. (1956) *J. Chem. Phys. 24*, 966−989.

Marcus, R. A., & Sutin, N. (1985) *Biochim. Biophys. Acta 811*, 265−322.

Margoliash, E., & Frohirt, N. (1959) *Biochem. J. 71*, 570−575.

Matthis, A. L., Vitello, L. B., & Erman, J. E. (1995) *Biochemistry 34*, 9991−9999.

Mauro, J. M., Fishel, L. A., Hazzard, J. T., Meyer, T. E., Tollin, G., Cusanovich, M. A., & Kraut, J. (1988) *Biochemistry 27*, 6243−6256.

Mei, H., Wang, K., McKee, S., Miller, M. A., Pielak, G. J., Durahm, B., & Millett, F. (1996) (submitted to *Biochemistry*).

Miller, M. A., Han, G. W., & Kraut, J. (1994a) *Proc. Natl. Acad. Sci. U.S.A. 91*, 11118−11122.

Miller, M. A., Liu, R.-Q., Hahm, S., Geren, L., Hibdon, S. Kraut, J., Durham, B., & Millett, F. (1994b) *Biochemstry 33*, 8686−8693.

Miller, M. A., Erman, J. E., & Vitello, L. B. (1995) *Biochemistry 34*, 12048−12058.

Miller, M. A., Geren, L., Han, G. W., Saunders, A., Beasley, J., Pielak, G. J., Durham, B., Millett, F., & Kraut, J. (1996) *Biochemistry 35*, 667−673.

Mondal, M. A., Fuller, H. A., & Armstrong, F. A. (1996) *J. Am. Chem. Soc. 118*, 263−264.

Moser, C. C., Keske, J. M., Warncke, K., Farid, R. S., & Dutton, P. L. (1992) *Nature 355*, 796−802.

Nuevo, M. R., Chu, H.-H., Vitello, L. B., & Erman, J. E. (1993) *J. Am. Chem. Soc. 115*, 5873−5874.

Pappa, H. S., Tajbaksh, S., Saunders, A. J., Pielak, G. J., & Poulos, T. L. (1996) *Biochemistry 35*, 4837−4845.

Pelletier, H., & Kraut, J. (1992) *Science 258*, 1748−1755.

Purcell, W. L., & Erman, J. E. (1976) *J. Am. Chem. Soc. 98*, 7033−7037.

Roe, J. A., & Goodin, D. B. (1993) *J. Biol. Chem. 268*, 20037−20045.

Scholes, C. P., Liu, Y., Fishel, L. A., Farnum, M. F., Mauro, J. M., & Kraut, J. (1989) *Isr. J. Chem. 29*, 85−92.

Scott, J. R., McLean, M., Sligar, S. G., Durham, B., & Millett, F. (1994) *J. Am. Chem. Soc. 116*, 7356−7362.

Sivaraja, M., Goodin, D. B., Smith, M., & Hoffman, B. M. (1989) *Science 245*, 738−74.

Smith, H. T., Ahmed, A. J., & Millett, F. (1981) *J. Biol. Chem. 256*, 4984−4990.

Summers, F. E., & Erman, J. E. (1988) *J. Biol. Chem. 263*, 14267−14275.

Vitello, L. B., Erman, J. E., Mauro, J. M., & Kraut, J. (1990) *Biochim. Biophys. Acta 1038*, 90−97.

Wang, J., Mauro, M., Edwards, S. L., Oatley, S. J., Fishel, L. A., Ashford, V. A., Xuong, N. H., & Kraut, J. (1990) *Biochemistry 29*, 7160−7173.

Wilcox, S. K., Jensen, G. M., Fitzgrald, M. M., McRee, D. E., & Goodin, D. B. (1996) *Biochemistry 35*, 4858−4866.

Zhou, J. S., Nocek, J. M., De Van, M. L., & Hoffman, B. M. (1995) *Science 269*, 204−207.

BI9611117